

Zinc adsorption on clays inferred from atomistic simulations and EXAFS spectroscopy

*Sergey V. Churakov\* and Rainer Dähn*

**Supporting information**

**3 Supplementary**

**1 Table**

**1 Figure**

**5 Pages**

## Supplementary 1

The structural formulas of the montmorillonite samples used in this work are<sup>1</sup>:

Milos:  $(\text{Si}_{7.76}\text{Al}_{0.24})(\text{Al}_{3.0}\text{Mg}_{0.54}\text{Fe(II)}_{0.02}\text{Fe(III)}_{0.44})\text{O}_{20}\text{OH}_4 \text{Na}_{0.79}$  (MW = 750.3 [g/mol])

STx-1:  $(\text{Si}_{7.91}\text{Al}_{0.09})(\text{Al}_{3.12}\text{Mg}_{0.75}\text{Fe(III)}_{0.14})\text{O}_{20}\text{OH}_4 \text{Na}_{0.84}$  (MW = 742.1 [g/mol])

Milos and STx-1 contain 1.26 wt% and 0.56 wt% Fe, respectively. Based on an XRD characterization of the montmorillonites used, no indications for crystalline Si-phases were detected. The < 0.5  $\mu\text{m}$  montmorillonite fraction used in this study was obtained in purification and conditioning processes. Briefly, the clay was thoroughly washed three times with 1 M  $\text{NaClO}_4$  to convert the clay into a homo-ionic Na form. The < 0.5  $\mu\text{m}$  size fraction was selected by successive washing with de-ionized water, combined with centrifugation and finally soluble hydroxyl-aluminum compounds and traces of amorphous iron were removed.

**Supplementary Table S1:** Experimental data and the chemical analysis of the filtered solutions for the samples prepared for P-EXAFS studies in 0.2  $\text{NaClO}_4$ .

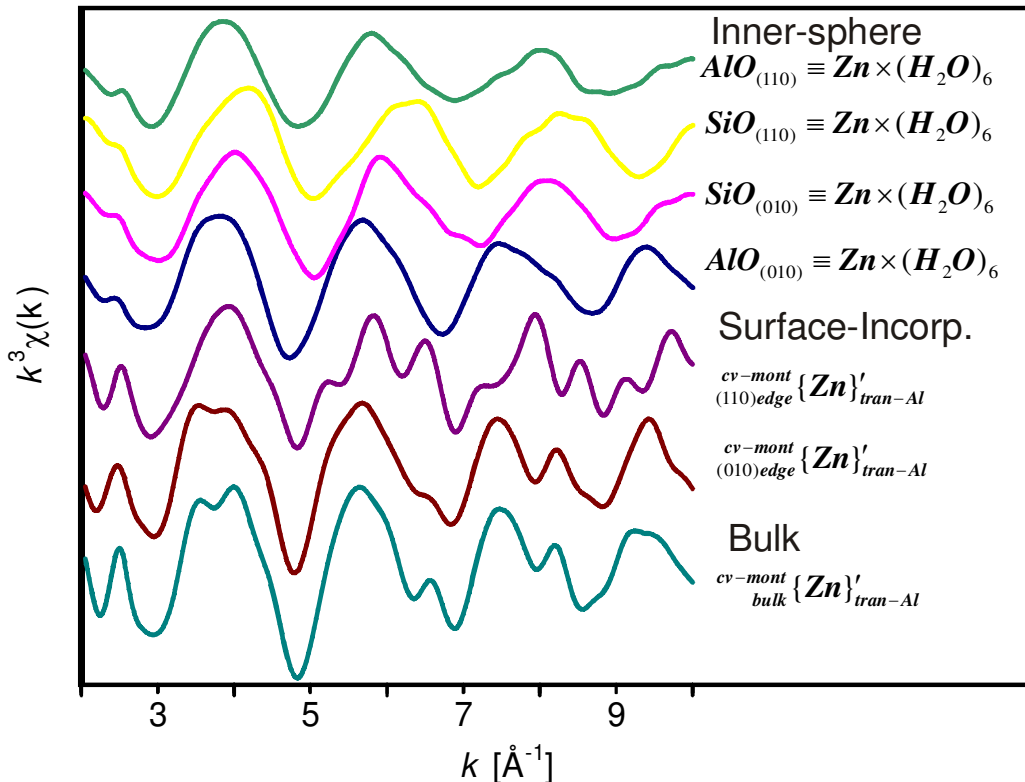
| Sample    | S:L<br>ratio<br>( $\text{g L}^{-1}$ ) | Initial Zn<br>conc.<br>(M) | Final Zn<br>conc.<br>(M) | Total Zn<br>sorbed<br>( $\text{mol kg}^{-1}$ ) | Si (M)               | Al (M)               |
|-----------|---------------------------------------|----------------------------|--------------------------|--|----------------------|----------------------|
| Milos-low | 2.0                                   | $5.0 \times 10^{-6}$       | $8.0 \times 10^{-7}$     | $2.7 \times 10^{-3}$                           | $2.8 \times 10^{-5}$ | $3.9 \times 10^{-6}$ |
| STx-1-low | 1.85                                  | $4.0 \times 10^{-6}$       | $4.6 \times 10^{-7}$     | $2.3 \times 10^{-3}$                           | $1.0 \times 10^{-4}$ | $2.8 \times 10^{-7}$ |

|                  |      |                      |                      |                      |                      |                      |
|------------------|------|----------------------|----------------------|----------------------|----------------------|----------------------|
| STx-1-<br>medium | 2.25 | $2.4 \times 10^{-4}$ | $1.7 \times 10^{-4}$ | $3.2 \times 10^{-2}$ | $1.1 \times 10^{-4}$ | $3.3 \times 10^{-7}$ |
|------------------|------|----------------------|----------------------|----------------------|----------------------|----------------------|

## Supplementary 2

In the GAPW method implemented in the QUICKSTEP module of the CP2K package, the Kohn–Sham orbitals are expanded using a linear combination of atom-centered Gaussian type orbital functions. In this study “short range” double- $\zeta$  polarized valence basis sets for all atoms in the systems were used<sup>8</sup>. This basis set was optimized for large scale simulations in condensed matter systems and was proved to give accurate structural results. The “soft” part of the electron charge density was expanded using an auxiliary basis set of plane waves up to a 200 Ry cutoff. The PBE exchange and correlation functional<sup>9</sup> used in this work is known to reproduce the structural properties of water accurately<sup>10</sup>. The dual space norm-conserving pseudopotentials<sup>11</sup> were applied to avoid explicit consideration of core electrons. Ab initio MD simulations based on the Born-Oppenheimer approximation were performed with a time step of 1.0 fs at 350K using the Nose-Hoover thermostat<sup>12, 13</sup>. Before each force evaluation step, the energy was converged to within a value of  $6 \times 10^{-10}$  au/atom using a single k-point in the origin of the Brillouin zone ( $\Gamma$ -point sampling only).

### Supplementary 3



**Supplementary Figure S1.** Basis components used for the fit of experimental spectra at low and medium loading.

### References

1. Vantelon, D.; Montarges-Pelletier, E.; Michot, L. J.; Briois, V.; Pelletier, M.; Thomas, F., Iron distribution in the octahedral sheet of dioctahedral smectites. An Fe K-edge X-ray absorption spectroscopy study. *Physics and Chemistry of Minerals* **2003**, 30, (1), 44-53.
2. Schlegel, M. L.; Manceau, A.; Charlet, L.; Chateigner, D.; Hazemann, J. L., Sorption of metal ions on clay minerals. 3. Nucleation and epitaxial growth of Zn phyllosilicate on the edges of hectorite. *Geochimica et Cosmochimica Acta* **2001**, 65, 4155-4170.
3. Schlegel, M. L.; Manceau, A.; Chateigner, D.; Charlet, L., Sorption of metal ions on clay minerals: 1. Polarized EXAFS evidence for the adsorption of Co on the edges of hectorite particles. *Journal of Colloid and Interface Science* **1999**, 215, 140-158.
4. Manceau, A.; Chateigner, D.; Gates, W. P., Polarized EXAFS, distance-valence least-squares modeling (DVLS) and quantitative texture analysis approaches to the

structural refinement of Garfield nontronite. *Physics and Chemistry of Minerals* **1998**, 25, 347-365.

5. Dähn, R.; Scheidegger, A. M.; Manceau, A.; Curti, E.; Baeyens, B.; Bradbury, M. H.; Chateigner, D., Th uptake on montmorillonite: A powder and polarized extended x-ray absorption fine structure (EXAFS) study. *Journal of Colloid and Interface Science* **2002**, 249, 8-21.

6. Dähn, R.; Scheidegger, A. M.; Manceau, A.; Schlegel, M. L.; Baeyens, B.; Bradbury, M. H.; Chateigner, D., Structural evidence for the sorption of Ni(II) atoms on the edges of montmorillonite clay minerals. A polarized X-ray absorption fine structure study. *Geochimica et Cosmochimica Acta* **2003**, 67, (1), 1-15.

7. Dähn, R.; Scheidegger, A. M.; Manceau, A.; Schlegel, M. L.; Baeyens, B.; Bradbury, M. H.; Morales, M., Neoformation of Ni phyllosilicate upon Ni uptake on montmorillonite: A kinetics study by powder and polarized extended X-ray absorption fine structure spectroscopy. *Geochimica et Cosmochimica Acta* **2002**, 66, (13), 2335-2347.

8. VandeVondele, J.; Hutter, J., Gaussian basis sets for accurate calculations on molecular systems in gas and condensed phases. *Journal of Chemical Physics* **2007**, 127, 114105

9. Perdew, J. P.; Burke, K.; Ernzerhof, M., Generalized gradient approximation made simple. *Physical Review Letters* **1996**, 77, (18), 3865-3868.

10. Grossman, J. C.; Schwegler, E.; Draeger, E. W.; Gygi, F.; Galli, G., Toward assessment of the accuracy of density functional theory for first principle simulations of water. *Journal of Chemical Physics* **2004**, 120, 300-311.

11. Goedecker, S.; Teter, M.; Hutter, J., Separable dual-space Gaussian pseudopotentials. *Physical Review B* **1996**, 54, (3), 1703-1710.

12. Hoover, W. G., Canonical dynamics: Equilibrium phase-space distributions. *Physical Review A* **1985**, 31, (3), 1695-1697.

13. Nose, S., A unified formulation of the constant temperature molecular dynamics methods. *Journal of Chemical Physics* **1984**, 81, (1), 511-519.